Available online at www.sciencedirect.com

ScienceDirect

Procedia Structural Integrity 2 (2016) 253–260

Structural Integrity Procedia

www.elsevier.com/locate/procedia

21st European Conference on Fracture, ECF21, 20-24 June 2016, Catania, Italy

Time dependent fracture behaviour of a carbon fibre composite based on a (rubber toughened) acrylic polymer

Tommaso Pini[a,]*, Francesco Briatico-Vangosa[a], Roberto Frassine[a], Marta Rink[a]

[a]*Dipartimento di Chimica, Materiali e Ing. Chimica "Giulio Natta", Politecnico di Milano, Piazza Leonardo da Vinci 32, Milano – 20133, Italy*

Abstract

The fracture behaviour of continuous carbon fibre laminates based on plain and rubber-toughened acrylic resins was investigated focusing on the influence of rate and temperature. The tensile behaviour of the two matrices was also characterized for subsequent analysis. In all cases the experimental window was extended by applying the time-temperature equivalence postulate. Fracture toughness at varying crack propagation rate turned out to have opposite trends for the two matrices. For the plain acrylic resin, a monotonically increasing trend with crack rate was found in agreement with viscoelastic fracture theories. For the rubber-toughened resin the change of the failure mechanisms occurring at the crack tip, resulted in a monotonically decreasing trend for increasing crack rate. Rate and temperature effects were analysed in terms of volumetric strain during tensile tests. Composites turned out to be more resistant to crack propagation than the relevant matrices in both cases. Delamination fracture toughness turned out to have the same dependence on crack rate for rubber toughened matrix only. For composites based on the plain resin, no effect of crack rate on delamination fracture toughness was observed.

Peer-review under responsibility of the Scientific Committee of PCF 2016.

Keywords: thermoplastic composites; viscoelastic fracture; volume strain; rubber toughening; yield mechanisms;

1. Introduction

Composite materials are nowadays widely used in structural applications for which weight reduction is a critical issue. The interlaminar fracture toughness of a composite material is a fundamental property to investigate when

* Corresponding author. Tel.: +39-2-23994711; fax: +39-2-7063-8173.
E-mail address: tommaso.pini@polimi.it

Peer review under responsibility of the Scientific Committee of PCF 2016.
10.1016/j.prostr.2016.06.033

designing components with a damage tolerant approach. In the light of this, thermoplastic polymeric matrices gained greater interest due to their properties: among other advantages, they show a better fracture behaviour in comparison to thermosets. In the present work two thermoplastic acrylic resins were studied, one plain and one toughened with rubber particles in order to increase the resistance to crack growth. Laminates were produced by infusion moulding at room temperature using in-situ polymerization, so as to avoid the issues related to the high viscosity of thermoplastic resins, even at very high temperature. Since the fracture in composites is strongly related to matrix properties (Jordan et al. (1989)), in the present work a special attention was paid to matrix characterization and investigation of its viscoelastic behaviour. The intent was to investigate the fracture toughness dependence to crack propagation rate, and to compare the experimental results with the viscoelastic theories developed which have been reviewed in (Bradley et al. (1998); Frassine et al. (1996)).

2. Materials

The materials studied in the present work were two types of acrylic resins developed by Arkema, namely:

- Elium®, named E from now on, which has a glass transition temperature of 125 °C.
- Elium Impact®, named from now on EI, toughened with an acrylic block copolymer under the tradename of Nanostrength® (10 wt%). The rubber inclusions have dimensions smaller than 50 nm. Glass transition temperatures are 125 °C and -25 °C for the rubbery phase.

Using these materials as matrices. unidirectional continuous fibre laminates were prepared using T700 12K carbon fibre (60 vol%) as reinforcement phase. The composites were prepared by infusion moulding from the liquid monomers.

3. Methods

3.1. Dynamic mechanical analysis

Tests were performed on specimens having dimensions of 45x6x2 mm on a TA RSA-3 dynamic mechanical analyzer adopting a three point bending configuration. Isothermal frequency sweep tests from 0.1 to 10 Hz, varying the temperature from -60 to 110 °C were conducted on both resins. Data were reduced to single master curves at the reference temperature of 23 °C by shifting single isothermal curves along the logarithmic time axis; hence, shift factors as a function of temperature were obtained.

3.2. Tensile tests

Uniaxial tensile tests were carried out at constant displacement rate on dumbbell specimens having gage dimensions of 18x5x2 mm. Temperature was varied from 0 to 60 °C, at each temperature tests at three displacement rates (0.1, 1 and 10 mm/min) were performed. Before testing, specimens were painted white and then a fine pattern of black speckles was applied by airbrushing. Water based paint was chosen in order to avoid any kind of interaction with the polymer which could have altered the results. Strains were measured by video recording the tests and then performing Digital Image Correlation. All tests were performed on an Instron 1121 machine equipped with a 10 kN load cell and a thermostatic cabinet.

Strain components were evaluated following the approach proposed by Heikens et al. (1981) and Franck and Lehmann (1986). Total volume strain is equal to:

$$\frac{\Delta V}{V_0} = \left(1+\varepsilon\right)\left(1+\varepsilon_{lat}\right)^2 - 1 \qquad (1)$$

where ε is the longitudinal strain and ε_{lat} is the lateral contraction, considered the same in both transversal directions. The elastic contribution to volume strain is found considering

$$\varepsilon_{el} = \sigma / E \qquad \varepsilon_{lat} = -\nu\varepsilon \tag{2}$$

in which σ is the applied stress, E is the Young's modulus and ν is the Poisson's ratio both determined close to the origin of the stress-strain curves. Substituting *(2)* into *(1)* and neglecting higher order terms:

$$\left(\frac{\Delta V}{V_0}\right)_{el} = \left(1-2\nu\right)\varepsilon_{el} \tag{3}$$

Assuming that volume strain components due to elasticity and crazing and/or cavitation are additive and that shearing does not involve an increase in volume, the contribution of crazing and/or cavitation to total volume strain is:

$$\left(\frac{\Delta V}{V_0}\right)_{cr/cav} = \left(\frac{\Delta V}{V_0}\right) - \left(\frac{\Delta V}{V_0}\right)_{el} = \left(\frac{\Delta V}{V_0}\right) - \left(1-2\nu\right)\varepsilon_{el} \tag{4}$$

The shear component, ε_{sh}, of longitudinal strain can be obtained from *(5)* assuming that the strain component due to crazing and/or cavitation, $\varepsilon_{cr/cav}$, is equal to the volume strain component $(\Delta V/V_0)_{cr/cav}$ and assuming also the additivity of longitudinal strain components:

$$\varepsilon = \varepsilon_{el} + \varepsilon_{cr/cav} + \varepsilon_{sh} \tag{5}$$

Yield point was chosen as the point at which a change in slope of the volumetric strain vs. applied strain curve was observed. Such point was found to be slightly before or almost coincident with the maximum of the stress curve in all the tests performed.

3.3. Fracture tests

Fracture tests on both neat resins and composites were performed on an Instron 1185 machine equipped with a 10 kN load cell and a thermostatic cabinet.

3.3.1. Neat resins

Fracture of neat resins was evaluated using double torsion test configuration (Fig. 1). This configuration was chosen for its experimental simplicity and the possibility of controlling the crack propagation rate (Evans (1972)). Tests were conducted at temperatures and displacement rates varying from 0 to 60 °C and 0.1 to 100 mm/min respectively. Specimens having dimensions of 120x45x6 mm and 200x70x10 mm, with initial notch lengths of 22.5 and 30 mm respectively, were adopted. For both geometries, a 60° V-groove, to a depth equal to 15% of the specimen thickness, was introduced on one side in order to prevent the crack from wandering.

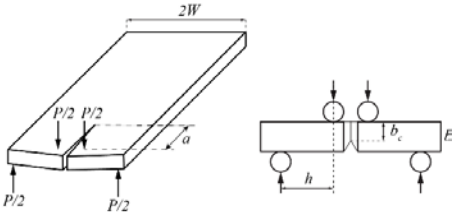

Fig. 1. Double Torsion test configuration

Fracture toughness was evaluated as:

$$G_{Ic} = \frac{P_c^2}{2b_c}\frac{\partial C}{\partial a} \tag{6}$$

where P_c is the load during crack propagation, b_c is the thickness of the grooved cross-section, C is the specimen compliance and a the crack length. The derivative of the compliance with respect to the crack length is equal to:

$$\frac{\partial C}{\partial a} = \frac{h^2}{2k_1 \mu W b^3} \tag{7}$$

where h is the arm length of applied moment, W is the width, b is the thickness, k_1 a correction factor and μ is the shear modulus. It can be noticed that $\partial C/\partial a$ is independent on the crack length, therefore is constant throughout the whole test. Generally the load remains constant during a certain stage of a double torsion test (Frassine et al. (1988)) during which the crack propagation speed can be expressed as

$$\dot{a} = \frac{\dot{x}}{P_c \dfrac{\partial C}{\partial a}} \tag{8}$$

thus it derives from *(6)* and *(8)* that both fracture toughness and crack propagation speed are constant, making the correlation of these two quantities very easy. The derivative of compliance calibration with respect to crack length can be evaluated from *(7)* or with an experimental calibration method, by measuring compliance of specimens having different crack lengths a at a given temperature and strain rate. If the geometry is kept constant in a test performed at different strain rate or temperature, the variation of the term $\partial C/\partial a$ is related only to the variation of the shear modulus, which can be evaluated from the ratio between the compliance of the tested specimen and the compliance of the calibration specimen. Corrections proposed by Leevers (1986) to take into account the reduction of the arm length of the applied moment at large displacement were adopted.

3.3.2. Composites

Interlaminar fracture toughness was investigated with Double Cantilever Beam test configuration according to ISO 15024 (Fig. 2). Tests were conducted at temperature and displacement rate varying from 0 to 60 °C and 0.2 to 200 mm/min respectively. Specimens having dimensions of 190x20x5 mm and 190x20x10 mm, with an initial delamination 60 mm long in both cases, were adopted. Strain energy release rate was calculated as follows:

$$G_{Ic} = \frac{3P_c\delta}{2W(a+|\Delta|)}\frac{F}{N} \tag{9}$$

in which P_c is the load, δ the displacement, W the width of the specimen, a the crack length and Δ, F, N are corrective factors for compliance, large displacements and load blocks stiffening respectively. The crack propagation was video recorded from the side of the specimen, previously painted white in order to have a good image contrast.

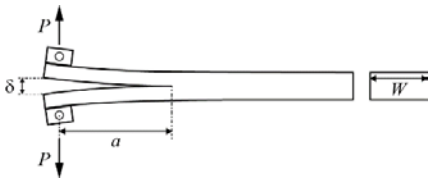

Fig. 2. Double Cantilever Beam test configuration

4. Results and discussion

4.1. Dynamic Mechanical Analysis

Master curves of conservative modulus vs. frequency were built shifting along the logarithmic time axis the isothermal curves obtained at different temperatures. Fig. 3 shows isothermal curves and the master curves for the reference temperature of 23 °C for E and EI matrix. The two master curves have similar shape but EI matrix has slightly lower values as expected in the presence of a rubbery phase.

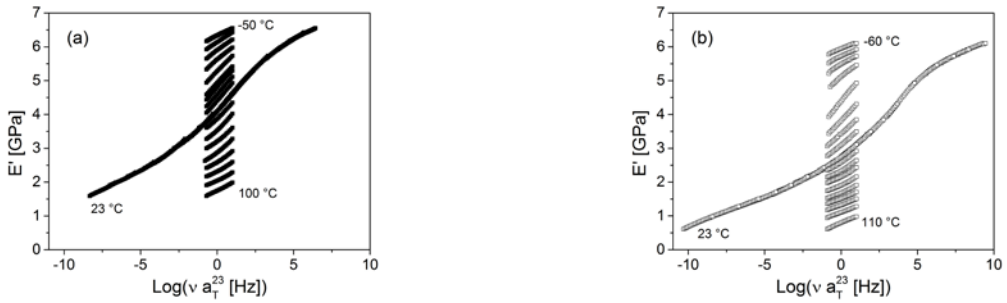

Fig. 3. Conservative modulus vs. frequency experimental isothermal curves and relevant master curves at the reference temperature of 23 °C for E (solid symbols) and EI (hollow symbols).

4.2. Tensile tests

Volumetric vs. longitudinal strain for EI matrix at different conditions of rate and temperature are shown in Fig. 4(a): at first, all curves display a similar slope related to the elastic volume strain then a higher slope is observed. Yield onset, as already mentioned, was supposed to occur at the strain where the slope changes. The slopes, after yield, give information on the damage mechanism acting (Bucknall et al. (1984); Coumans et al. (1980); Franck and Lehmann (1986)): in the case of pure crazing the slope is equal to 1 while in the case in which only shear occurs the slope is 0, while cavitation of the rubber domains gives rise to low values of volume dilatation and promotes shear yielding. For EI matrix, the slopes, after yield, increase with increasing strain rate and decreasing temperature varying between 0.15 and 0.75.

Fig. 4(b) and Fig. 4(c) show the strain components due to crazing and/or cavitation and shear respectively: at a given strain, as temperature increases (or strain rate decreases) the strain component linked to volume changes decreases while the shear component increases indicating that probably the damage mechanism tends to switch from crazing to cavitation and shearing. For the E matrix, non-elastic volume changes were very small.

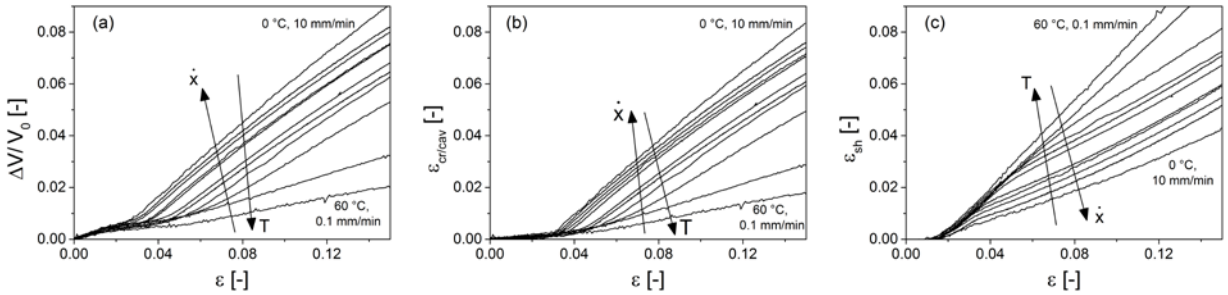

Fig. 4. Volumetric strain (a), crazing and/or cavitation (b) and shear (c) contributions to longitudinal strain vs. longitudinal strain for EI matrix

Yield stress vs. time to yield curves at different temperatures and rates are shown in Fig. 5 along with the master curves obtained shifting the data along the logarithmic time axis.

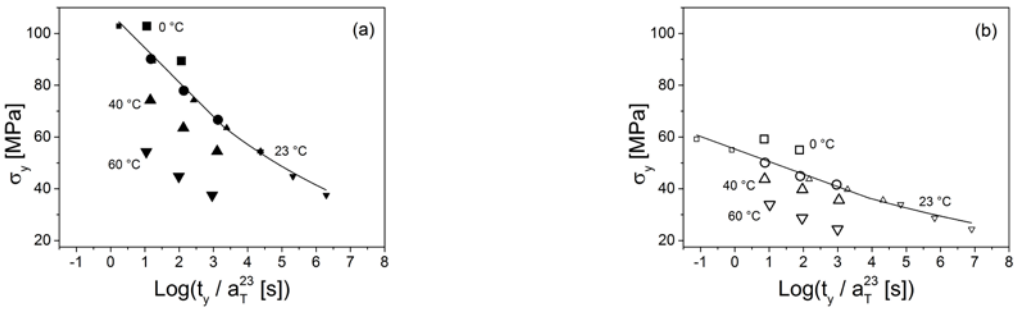

Fig. 5. Yield stress vs. time to yield isothermal curves (larger symbols) and relevant master curves (smaller symbols) at the reference temperature of 23 °C for E (solid symbols) and EI (hollow symbols) matrices Solid lines are power laws fittings.

4.3. Fracture tests

Results from double torsion tests, performed at different rates and temperatures, are shown in Fig. 6 for E and EI matrices. Master curves, obtained by shifting the data along crack speed axis, are reported also. Fig. 7 shows the shift factors obtained from small strains, yield and fracture data. They are all very similar, only the shift factors relevant to fracture of E matrix are slightly different. The dependence of fracture toughness on crack propagation speed is different for the two matrices. In the case of E matrix, an increasing trend is observed. Following Williams and Marshall's approach as reported in (Bradley et al. (1998)), fracture toughness is equal to

$$G_{Ic} = \delta_c \sigma_y(t_\alpha) \tag{10}$$

where δ_c is the crack opening displacement, considered constant, and $\sigma_y(t_\alpha)$ is the yield stress at a time comparable with that necessary for the crack to grow across the process zone. Considering the size of the process zone given by Dugdale's crack tip model and in the hypothesis that relaxation modulus vs. time and yield stress vs. time to yield can be described by power laws with exponents m and n respectively, fracture toughness dependence on crack propagation speed follows a power law:

$$G_{Ic} \propto \dot{a}^{\frac{n}{1+m-n}} \tag{11}$$

Fitting power laws to the data of Fig. 3(a), with $t = 1/(\pi^2 v)$, and Fig. 5(a), the exponent calculated from (11) is in good agreement to that of the power law fitted to the fracture toughness vs. crack propagation speed experimental data from Fig. 6(a).

As for the EI matrix, a decreasing trend with increasing crack propagation speed, which cannot be described by the viscoelastic fracture theories, was observed. It has been related to a change in the deformation mechanism at the crack tip as crack propagation speed increases. The high toughness observed at low crack speeds could be associated to cavitation and shear, which were observed at low strain rate (or high temperature) in tensile tests, while the lower values at high crack speeds to crazing, which was the main mechanism at high strain rate (or low temperature).

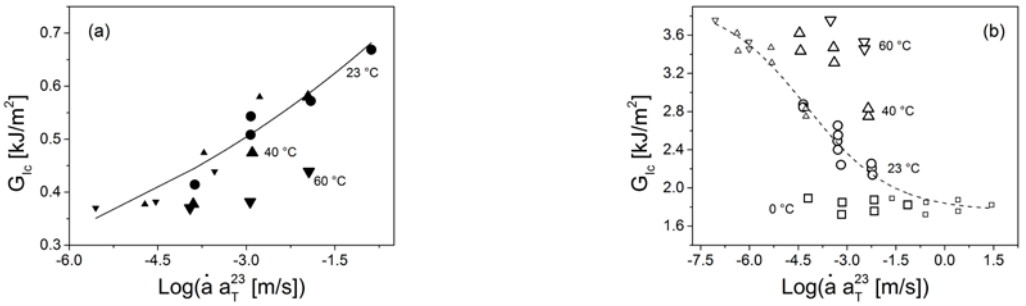

Fig. 6. Fracture toughness vs. crack propagation speed isothermal curves (larger symbols) and relevant master curves (smaller symbols) at the reference temperature of 23 °C for E (solid symbols) and EI (hollow symbols) matrices. Solid lines are power laws fittings, dashed lines are visual aids.

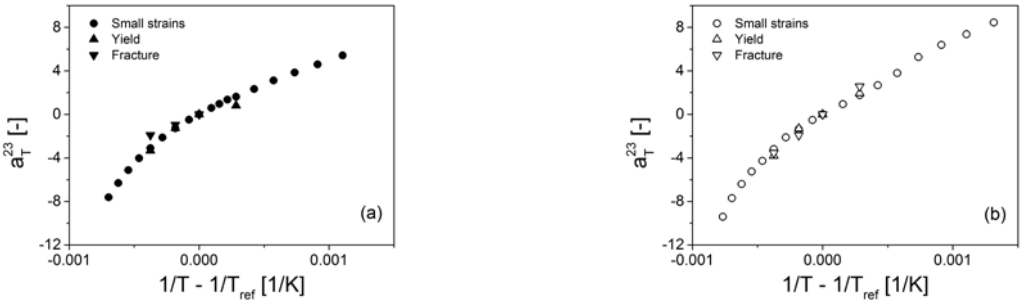

Fig. 7. Shift factors obtained at small strains (DMA), yield (tensile tests) and fracture (DT) for E (solid symbols) and EI (hollow symbols) matrices at the reference temperature of 23 °C.

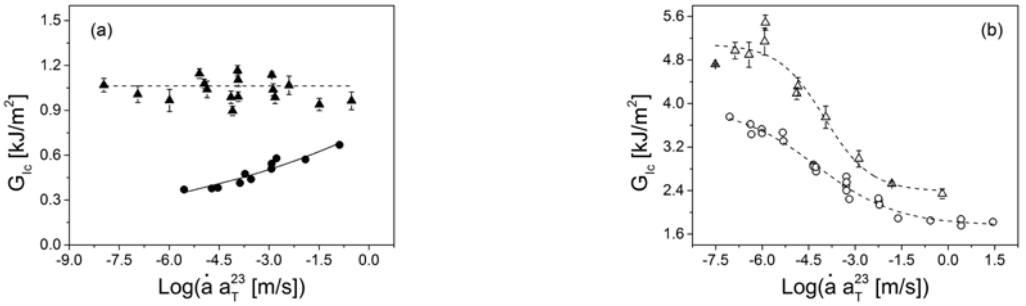

Fig. 8. Fracture toughness vs. crack propagation speed master curves for E matrix (solid circles), E matrix based composite (solid triangles), EI matrix (hollow circles), EI matrix based composite (hollow triangles) at the reference temperature of 23 °C. Solid lines are power laws fittings, dashed lines are visual aids.

Fig. 8 shows the composites fracture toughness vs. crack propagation speed master curves, obtained using the shift factors of the relevant matrices. Master curves of the matrices are also shown for comparison. The dependence of G_{Ic} on crack propagation speed of the composites reflects that of the matrix for EI, while in the case of E matrix the energy release rate does not show, within experimental data scattering, a significant rate dependence.
In both cases, fracture toughness of the laminates is higher than that of the corresponding neat resin, indicating that no physical constraint to the development of the process zone induced by the fibres, which may in some cases lead to a just partial transfer of toughness from the matrix to the composite, occurs. The large, additional dissipation of energy is probably introduced by fibre-related damage mechanisms, such as fibre bridging which was clearly observed during the tests

5. Concluding remarks

The two resins studied showed a very different dependence of fracture toughness on crack propagation rate. The increasing trend observed for the E matrix complies with viscoelastic fracture theories, for which the strain energy release rate dependence on crack speed is controlled by the viscoelasticity of the material. On the other hand, the toughened resin showed a decreasing trend of fracture toughness with increasing crack propagation speed, which, based on tensile tests results, was related to the different toughening mechanisms, promoted by the rubber particles, occurring at different crack speeds. In this case, a larger volume of material at the crack tip is involved in energy dissipating mechanisms; hence, the local energy dissipation variation at varying the crack rate may mask the effect of viscoelasticity of the bulk material.

Composite materials prepared by infusion moulding with E and EI matrices, showed an interlaminar fracture toughness much higher than that of the relevant neat resins. The dependence of fracture toughness on crack propagation speed for the composites is slightly different from that of the relevant matrices, due to the contribution given by the fibres, which may be different at the different crack speeds or temperatures.

Acknowledgements

The Authors gratefully acknowledge the contribution of Dr. Pierre Gerard of the Groupement de Recherche Arkema in Lacq (France) for providing the materials of the present research and for many lively discussions on the results.

References

Bradley, W., Cantwell, W.J., Kausch, H.H., 1998. Viscoelastic creep crack growth: a review of fracture mechanical analyses. Mechanics of Time-Dependent Materials 1, 241-268.

Bucknall, C.B., Partridge, I.K., Ward, M.V., 1984. Rubber toughening of plastics. Part 7 Kinetics and mechanisms of deformation in rubber-toughened PMMA. Journal of Materials Science 19, 2064-2072

Coumans, W.J., Heikens, D., Sjoerdsma, S.D., 1980. Dilatometric investigation of deformation mechanisms in polystyrene-polyethylene block copolymer blends: correlation between Poisson ration and adhesion. Polymer 21, 103-108.

Evans, A.G., 1972. A method for evaluating the time-dependent failure characteristics of brittle materials - and its application to polycrystalline alumina. Journal of Materials Science 7, 1137-1146.

Frank, O., Lehmann, J., 1986. Determination of various deformation processes in impact-modified PMMA at strain rates up to 10^5%/min. Colloid & Polymer Science 264, 473-481.

Frassine, R., Riccò, T., Rink, M., Pavan, A., 1988. An evaluation of double-torsion testing of polymers by visualization and registration of curved crack growth. Journal of Materials Science 23, 4027-4036.

Frassine, R., Rink, M., Leggio, A., Pavan, A., 1996. Experimental analysis of viscoelastic criteria for crack initiation and growth in polymers. International Journal of Fracture 81, 55-75.

Heikens, D., Sjoerdsma, S.D., Coumans, W.J., 1981. A mathematical relation between volume strain, elongational strain and stress in homogeneous deformation. Journal of Material Science 16, 429-432.

Jordan, W.M, Bradley, W.L., Moulton, R.J., 1989. Relating resin mechanical properties to composite delamination fracture toughness. Journal of Composite Materials 23, 923-943.

Leevers, P.S., 1986. Large deflection analysis of the double torsion test. Journal of Materials Science 5, 191-192.